Aquatic Geochemistry (2024) 30:31–48
https://doi.org/10.1007/s10498-024-09423-w

ORIGINAL ARTICLE

Direct Salinity Effect on Absorbance and Fluorescence of Chernozem Water-Extractable Organic Matter

Vladimir A. Kholodov[1,3] · Natalia N. Danchenko[1] · Aliya R. Ziganshina[1] · Nadezhda V. Yaroslavtseva[1] · Igor P. Semiletov[2,3]

Received: 5 August 2023 / Accepted: 31 January 2024 / Published online: 24 February 2024

Abstract

Soil-derived dissolved organic matter (DOM) has a significant impact on aquatic ecosystems. Identifying the fluorescence signatures of DOM from different soils in river and sea waters can provide valuable insights into its migration patterns. This makes crucial assessing the contributions of pH, salinity, and other milieu parameters to the variability of DOM optical properties. Present study investigates the changes in DOM of Chernozems under varying salinity using UV–visible absorbance spectroscopy and 3D-fluorescence spectroscopy coupled with parallel factor analysis (EEMs-PARAFAC). Water-extractable organic matter (WEOM) extracted from soils of two field experiments of contrasting land use: long-term bare fallow (LTBF) and annually mown steppe (Steppe), was used as a proxy for DOM. Diluted extracts were incubated with varying NaCl concentrations in the dark and then examined. Steppe WEOM exhibited fair constancy of optical parameters under increasing salinity, while significant changes of the optical indices and of PARAFAC components's loadings were observed for LTBF WEOM. The remarkable stability of the Steppe WEOM can be attributed to its chemical diversity. Two distinct and sufficiently stable humic-like PARAFAC components have the potential to serve as markers of Chernozem DOM. The findings clearly demonstrate that salinity itself slightly reduces absorption and fluorescence and changes some optical indices of WEOM of Chernozems.

Keywords Chernozem · DOM · UV–Vis absorbance · EEMs-PARAFAC · staRdom · Fluorescence component

✉ Natalia N. Danchenko
nataly_danch@mail.ru

[1] Dokuchaev Soil Science Institute, Pyzhevsky Lane, 7/2, Moscow, Russia 119017

[2] Ilyichov Pacific Oceanological Institute, Far Eastern Branch of the Russian Academy of Sciences, Vladivostok, Russia

[3] National Research Tomsk Polytechnic University, Tomsk, Russia

1 Introduction

Soil is the largest terrestrial reservoir of organic carbon (OC), containing more than 1500 Pg C in the top 100 cm layer, which is triple the amount of C in all aboveground biomass (Batjes 2014). DOM, comprising a small fraction of soil organic matter (OM), represents the most active, accessible, and mobile pool, participating in numerous soil processes. It serves as a substrate for organisms, influences the bioavailability and transport of trace elements and xenobiotics, and affects the stability of soil colloids and aggregates (Zsolnay 1996; Kalbitz et al. 2000; Chantigny 2003; Karavanova 2013; Rodrigues et al. 2015; Gmach et al. 2020). DOM migration through the soil profile impacts groundwater and surface water quality. Once in the hydrosphere, soil C is further transported by river networks delivering about two-thirds of its C to inland waters and the remainder—to the ocean (Cole et al. 2007; Bianchi 2011). The global flux of dissolved organic carbon (DOC) from land to ocean via rivers is estimated at about 0.2 Pg C per year and forms the bulk of the oceanic carbon cycle (Raymond and Spencer 2015). The amount and composition of terrigenous DOM influence microbial growth, benthic respiration, and carbon dioxide emissions from water bodies (Findlay et al. 2001; Piscart et al. 2009; Bengtsson et al. 2018), making soil-derived DOM significant as a global ocean carbon source.

Along the pathway, DOM undergoes significant changes due to the exposure of sunlight irradiation and degradation by aquatic microbiota (Raymond and Spencer 2015). The specific mechanisms of terrigenous OM transformation in hydrosystems are the focus of many studies, but their cumulative effects are still hard to predict (Mostofa et al. 2011; Bengtsson et al. 2018). However, recent studies have shown that soil DOM can be relatively resistant to photo- and biodegradation (Hansen et al. 2016), detectable in marine and oceanic waters, and used as markers of terrigenous fluxes (Walker et al. 2013; Mann et al. 2016; Eder et al. 2022). In various soils types, DOM exhibits substantial compositional and structural variations, providing an opportunity to determine the origin of DOM transported over long distances. Isolating the OM signals of specific soil types in riverine and then in marine waters can facilitate tracking the migration of terrigenous carbon in plumes, enabling the development of more reliable models of global ocean flows and climate changes (Osadchiev et al. 2020).

UV–Vis absorbance and excitation–emission matrices of fluorescence spectroscopy coupled with parallel factor analysis (EEMs-PARAFAC) are widely used to characterize quality of DOM from various sources. These methods offer high sensitivity, allow analysis of minimally altered samples, and provide abundant compositional information (Stedmon et al. 2003; Coble et al. 2014). The use of optical measurements, which can be rapidly collected and measured, is one pathway that can help to capture changes in terrigenous DOM supply and examine how it may alter under future scenarios with sufficient temporal and spatial resolution (Mann et al. 2016; Osburn et al. 2014). Recent years have witnessed the accumulation of extensive libraries of such data (Murphy et al. 2014). However, to understand whether DOM fluorescence varies due to different origins or to the influence of pH, salinity, dissolved oxygen content, etc., deeper studies of the relationships between fluorescence and aquatic conditions are required (Ishii and Boyer 2012). Water salinity (ionic strength) is one of the important abiotic factors influencing OM conformation hence the optic properties of DOM (Boyd et al. 2010; Osburn et al. 2014). While a lot of studies have explored spatial and temporal variations of DOM optic properties in estuarine and inland waters with various salinities (Provenzano et al. 2008; Bianchi 2011; Walker et al. 2013; Osburn et al. 2014 and refs therein; Amaral et al. 2021), only a limited number of studies

have directly assessed their modifications as influenced by salinity (Esteves et al. 1999; Boyd et al. 2010; Gao et al. 2015; Cuss et al. 2019).

In this study, we investigate the impact of salinity on the optical properties and structural characteristics of Chernozem DOM using afore-mentioned optical methods combined with PARAFAC. Two samples of Chernozem of contrasting land uses were selected: steppe — undisturbed soil containing the most diverse OM and bare fallow — maximally plowed soil, with much more homogeneous and stable OM. As a laboratory proxy of DOM, we used a water-extractable organic matter (WEOM), which is very close to DOM in composition (Zsolnay 1996; Chantigny 2003).

2 Materials and Methods

2.1 Study Area and Sample Collection

The samples were collected in the Kursk region (Central Chernozem Zone of Russia). The climate in this area is temperate with a mean annual temperature + 5.3 °C and mean precipitation of 550 mm. The soil type is Protocalcic Chernozems (WRB, 2015), clay loam on loamy loesses. Two contrasting land use units from long-term field experiments were selected for soil sampling.

(1) Permanent long-term (since 1964) bare fallow (hereafter — LTBF) plot of the field station of the Kursk Federal Agrarian Scientific Center (51° 37′ 17″ N 36° 15′ 44″ E). The plot is annually plowed without sowing or weeding, resulting in a lack of fresh organic matter input to the soil for over 50 years. As a result, the LTBF soil is depleted of organic carbon (OC) and contains extremely recalcitrant and minimally diverse organic matter (Barré et al. 2010; Menichetti et al. 2015; Franko and Merbach 2017; Kholodov et al. 2020a, b).
(2) Annually mowed steppe (hereafter — Steppe) plot located in the protected Streletskaya steppe of the Central Chernozem State Biosphere Reserve after V.V. Alekhin (N 51° 34′ 12.0″ N 36° 05′ 27.0″ E). This soil may be considered as undisturbed Chernozem and is enriched with OC, exhibiting maximum diversity of its OM composition.

For each location, we took samples from the top layer (0–15 cm) in three replicates. To reduce uncertainty related to aggregate composition heterogeneity, a 1–2 mm size fraction was selected from air-dried samples by sieving. This fraction is the most contributing to the carbon content in typical Chernozem and shows the least variability (Kholodov et al. 2019).

2.2 WEOM Extraction

The 1–2 mm aggregates were ground in a porcelain mortar and sieved on a size below 1 mm prior to extraction. WEOM was extracted according to the previously described method (Kholodov et al. 2020a). Briefly, ultrapure deionized water (ASTM Type 1, 18.2 MΩ-cm) was added to the soil aliquot at a ratio of 5:1 (water: soil) by mass and mixed on an orbital shaker for eight hours. After extraction samples were centrifuged for 10 min at 11,000 g, and the supernatant was decanted and filtered through 0.22 µm cellulose filters to

exclude most microbial activity. The resulting WEOM were stored at + 4 °C and processed within two weeks of preparation.

2.3 Incubation Under Various Salinities

2.3.1 Preparation of the Stock Sodium Chloride Solution

Before using reagent-grade crystalline sodium chloride (NaCl) was purified of organic carbon by calcination in a muffle furnace at a 400 °C for four hours before use. The purity of the stock solution (100 g/L) was confirmed by low absorbance (< 0.02) in the 200–260 nm range.

2.3.2 Experimental Procedure

For the incubation, we put 5 ml of the Steppe WEOM sample or 10 ml of the LTBF WEOM to 50 ml graduated centrifuge tubes. Then, the aliquots of stock NaCl-solution were added to obtain solutions with the final salt concentrations of 0, 1, 10, 20, and 35 g/L. The samples were brought to the mark with deionized water and mixed thoroughly. The final DOC content in the Steppe WEOM was 21 mg/L, while for the LTBF WEOM, it was 12 mg/L. The dilutions were made to minimize the inner filter effect during the acquisition of fluorescence spectra (Ohno 2002; Kothawala et al. 2013) based on preliminary UV absorbance measurements. Three replicates of each salinity level were prepared for both land use units. The tubes containing the solutions were kept at room temperature for 1 day in the dark (to avoid photooxidation). After incubation, the solutions were centrifuged for 10 min at 11,000× g. The supernatant was used for DOC content measurements and absorption and fluorescence spectra recording. Since the spectra acquisition took two working days, the samples were stored at + 4 °C and centrifuged immediately before measurements.

2.4 Determination of Organic Carbon Concentration

Dissolved organic carbon content of the initial extracts and experimental solutions was measured using Shimadzu TOC-L CSN analyzer (Japan) in the NPOC (non-purgeable organic carbon) mode. The instrument was calibrated with a series of potassium hydrophthalate standard solutions diluted according to a preliminary estimate of the C content in the samples. For each sample, the result was the average of at least two inputs that were satisfactory in terms of standard deviation (< 0.2) and coefficient of variation (< 3%). The initial WEOM extracts exhibited DOC content of 213 mg/L for Steppe and 62 mg/L for LTBF soil.

2.5 Spectral Measurements

UV–visible absorption spectra were recorded on a Shimadzu UV-1800 spectrophotometer in the 200–800 nm range with 1 nm step at a constant 1 nm slit width. The scanning rate was set 1500 nm/min. WEOM absorption spectra were recorded in 1 cm quartz cuvette against ultrapure water placed in the second optical channel of device. To calculate the optical parameters, the units of absorbance were converted into Napierian absorption coefficient a using the formula (Helms et al. 2008):

$a = 2.303A/l$, where a and A are the absorption coefficient (m^{-1}) and UV absorbance, respectively, and l is the optical path length (m).

Fluorescence spectra were recorded as excitation–emission matrices (EEMs) using the Shimadzu Spectrofluorophotometer RF-6000 at excitation and emission slit width 5 nm. The excitation wavelength ranged from 220 to 480 nm in 2 nm increments, while the emission range was 300–550 nm in 5 nm increments. The scan speed was maintained at 2000 nm/min, and the detector was set to low sensitivity. Blank fluorescence of ultrapure water was recorded at the beginning, middle, and end of each acquisition series. The pH of the initial extracts were 6.4 and 6.6 for LTBF and Steppe soils, respectively. The narrow pH range ensured no significant effects on fluorescence (Borisover et al. 2012).

2.6 Data Processing

The EEMs and absorbance spectra were processed using the staRdom package in the free R software environment (Pucher et al. 2019, www.r-project.org). The processing included instrumental spectrum correction, solvent subtraction (ultrapure water), inner filter correction, conversion to Raman units, Raman and Rayleigh scattering subtraction, interpolation, and calculation of the following indices (Murphy et al. 2013; Pucher et al. 2019):

$SUVA_{254}$ — a specific absorption at 254 nm, calculated by dividing the absorption coefficient at 254 nm (a_{254}) by the DOC concentration, characterizes the enrichment of chromophores — fragments with conjugated and aromatic bonds.

$S_{275\text{-}295}$ and $S_{350\text{-}400}$ — spectral slopes in the ranges of 275–295 and 350–400 nm, determined by approximating the absorption spectra with a monoexponential (decay) function:

$$a_\lambda = a_{\lambda \mathrm{ref}} e^{-S(\lambda - \lambda_{ref})}$$

where a_λ is the absorption coefficient at the corresponding wavelength (m^{-1}); λ is the wavelength (nm); λ_{ref} is the reference wavelength (nm); and S is the spectral slope (nm^{-1}). The slopes correlate with the apparent molecular size and aromaticity of WEOM. The spectral ratio (S_R), which is the ratio of $S_{275\text{-}295}$ to $S_{350\text{-}400}$, negatively correlates with DOM hydrophobicity and molecular weight (Twardowski et al. 2004; Helms et al. 2008).

FI (fluorescence index) — 450/500 nm emission intensities ratio at 370 nm excitation. A ratio greater than 1.9 indicates the dominance of organic matter of aquatic and microbial origin, while a ratio less than 1.4 suggests terrestrial organic matter (McKnight et al. 2001). In the context of soil, this index should be interpreted as a measure of organic matter transformation.

BIX (biological index) — the ratio of emission intensities at 380 nm and 430 nm wavelengths at an excitation of 310 nm. It characterizes the proportion of fresh organic matter of microbial origin. In natural waters, BIX > 1 indicates the predominance of autochthonous organic matter in DOM composition (Huguet et al. 2009).

HIX (humification index) is calculated from the ratio of the integral intensity of fluorescence emission in the 435–480 nm range to that in the 300–345 nm range at an excitation wavelength of 254 nm. This index characterizes structure complexity and condensation (H/C ratio) of DOM (Zsolnay et al. 1999).

To discriminate individual fluorescent components of soil WEOM, EEMs were decomposed by PARAFAC. The PARAFAC model was validated using the split-half method and residual analysis (Murphy et al. 2013; Pucher et al. 2019).

All the data were subjected to two-way analysis of variance (ANOVA) for salinity and land use factors. Post hoc multiple comparisons (Tukey's test) were performed at $p < 0.05$ using free R software.

3 Results and Discussion

3.1 Carbon Content in Samples of Different Salinity

The organic carbon content in the Steppe WEOM is almost 2.5 times higher than in LTBF WEOM, which is consistent with the total carbon content in the aggregates of the studied soils: 5.7 and 2.8%, respectively (Kholodov et al. 2020a). The proportion of WEOM carbon to the total soil organic carbon is 1.1% for LTBF and 1.9% for the Steppe, indicating a higher hydrophility and diversity of the Steppe OM. These figures fall within the range reported for the share of WEOM in total soil organic carbon (Zsolnay 1996).

Analysis of variance of DOC content data showed no significant differences in its content for prepared WEOM extracts after incubation at different salinities. That is the concentration of NaCl up to 35 g/L does not lead to a noticeable coagulation of WEOM of both Chernozems. In contrast, Esteves et al. observed a decrease in DOC concentration in freshwaters after incubation with the freeze-dried sea salt (Esteves, et al. 1999). Thus, the Chernozem WEOM appears to be quite stable in solution even at high salinity, at least, when it is due to the presence of alkali metal ions only.

3.2 Absorption Spectra and Spectral Indexes

The absorption spectra of the LTBF and Steppe WEOM samples change in different ways with increasing salinity. The UV range absorption clearly decreases for the former and shows subtle change for the latter (Fig. 1).

Two-way ANOVA showed that a_{254}, $S_{350\text{-}400}$ and S_R depend significantly on both soil type and salinity. Since DOC does not change significantly with increasing salinity, and photobleaching is excluded by incubation in the dark, the changes in the LTBF WEOM spectra are most likely caused by the OM conformational reorganization in response to the ionic strength raise. At higher salinity, the charges of ionized functional groups are shielded, reducing the repulsion between them. Additionally, the salting out effect occurs: hydrophobic components (fragments) close to compensate for the increase in free energy of system due to water structuring by electrolyte ions. This leads to a decrease in the solubility of non-electrolytes at a high electrolyte concentrations (Endo et al. 2012). The combined action of these two mechanisms results in the contraction and increased compactness of molecules/supramolecules adopting a spherocolloidal configuration, and masking some chromophores inside it (Ghosh and Schnitzer 1980; Patel-Sorrentino et al. 2002). This is probably the reason for the drop in the absorption intensity of LTBF WEOM.

$SUVA_{254}$ and S_R values for the LTBF WEOM indicate its greater aromaticity, hydrophobicity and molecular weight compared to the Steppe WEOM, with their values changing differently with salinity (Fig. 2). For the LTBF WEOM, a_{254} and $SUVA_{254}$ almost monotonically decreased as salinity increased (from 25 to 19 and from 2.2 to 1.55, respectively), while no significant changes were noticed for the Steppe WEOM. The different behavior seems to be due to the fact that LTBF SOM is more mature and hydrophobic, enriched with aromatic structures (Danchenko et al. 2020, 2022), and depleted of products of microbial

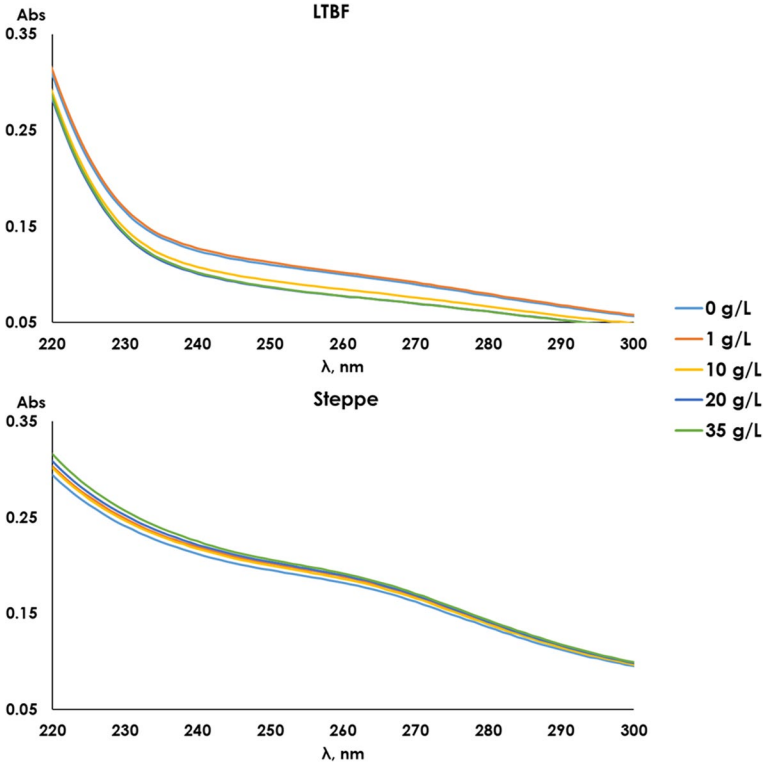

Fig. 1 Absorption spectra in the UV range at different solution salinities for WEOM samples of LTBF and Steppe

origin (Zhelezova et al. 2017). This evidenced by the wider C/N ratio of this sample. A study (Kholodov et al. 2020b) found that the LTBF soil organic matter differs from the Steppe soil organic matter in terms of lower diversity of its chemical components, which is likely true for WEOM as well. As mentioned earlier, this may explain the higher sensitivity of LTBF WEOM structure to salinity variations, which is reflected in the changes in optical characteristics.

In contrast, the Steppe WEOM is highly diverse due to the regular input of fresh plant residues, root exudates, and microbial products, enriching it with hydrophilic and surface-active compounds. These compounds probably compensate for the salting out effect and provide greater conformational and aggregation stability as salinity increases, hindering the realization of the mechanism proposed for LTBF WEOM. As a result, chromophores of steppe WEOM are less sensitive to changes in ionic strength.

Contrary to our findings (Gao et al. 2015) observed a slight increase in absorbance of commercial surface water humic preparations with increasing ionic strength of the solution.

The S_R index, which negatively correlates with the hydrophobicity and molecular weight of the DOM (Helms et al. 2008), decreases for LTBF samples as the salt concentration rises indicating an increase in hydrophobicity and average molecular weight (hydrodynamic radius) of the DOM. The apparent increase in WEOM molecular weight may be attributed to partial aggregation.

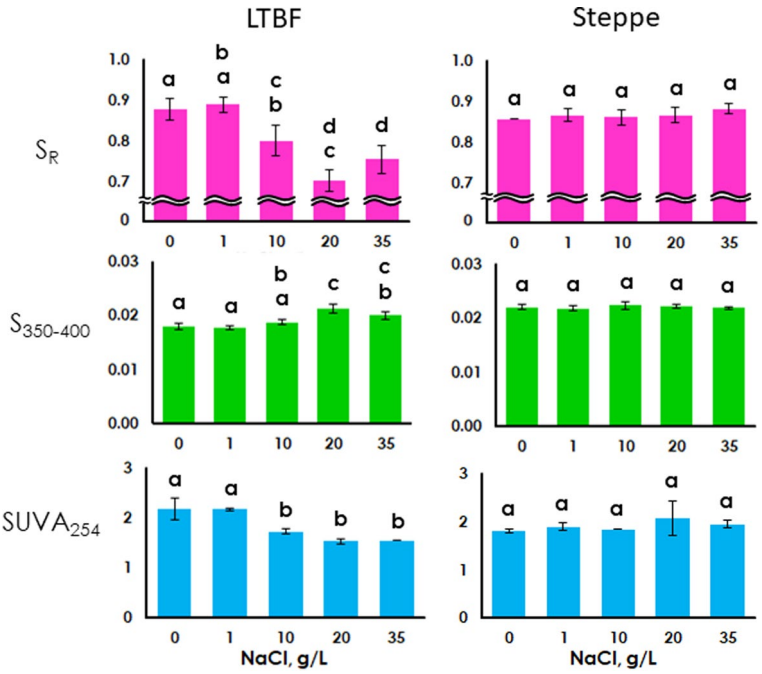

Fig. 2 LTBF and Steppe WEOM optical indexes as a function of salinity

Overall, the optical descriptors a_{254}, $SUVA_{254}$, $S_{350-400}$, and S_R and, consequently, WEOM structure of Chernozem with the most transformed OM (LTBF) respond to an increase in salinity, while the structure of the Steppe WEOM is almost unaffected by the ionic strength increase.

3.3 Fluorescence Spectra and Structural Indices Calculated from them

Fluorescence emission spectra intensity decreases with increasing salinity for both studied samples (Fig. 3). Probable mechanisms of fluorescence quenching in high ionic strength solutions are intramolecular rearrangements and ionization suppression (Osburn et al. 2014) result in shielding of some fluorophores inside the spherocolloidal DOM configuration (Patel-Sorrentino et al. 2002). A clear decrease in the fluorescence intensity of DOM in response to salinity growth was also observed for DOM samples extracted from increasingly saline soils (Provenzano et al. 2008) and for some DOM fractions of natural waters of different salinity (Boyd et al. 2010). However, those works use the samples taken from different locations and the changes in fluorescence intensity can probably be related not only to the increase in salinity, but also, for example, to variations in sources and the microbiota composition. It has been convincingly demonstrated in the study (Cuss et al. 2019) that changes in salinity do not explain the variability in fluorescence between saline groundwater DOM (discharging into the river) and river DOM.

The shape of the fluorescence spectra depends little on salinity but clearly differs between the LTBF and Steppe samples (Fig. 3). The intensities in the regions attributed to fluorophores of different nature depend more on the origin of the organic matter

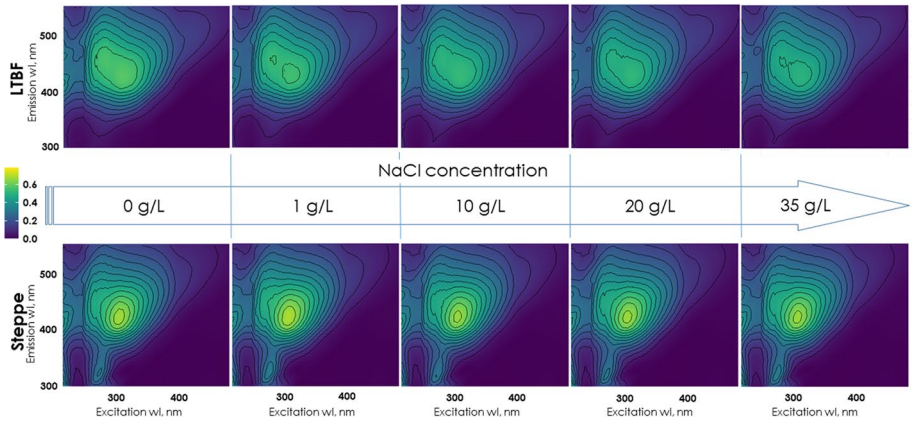

Fig. 3 Change in the fluorescence spectra intensity of LTBF WEOM (upper row) and Steppe WEOM (lower row) depending on the solution salinity

than on salinity (Supporting Information), as reflected by the values and trends in the change of structural descriptors calculated from EEM data, such as HIX, BIX, and FI.

The HIX index was expectedly high for the LTBF WEOM samples ranging from 10.8 to 12.8 and much lower for the Steppe ranging from 3.12 to 3.84. The higher HIX values obtained for LTBF WEOM are consistent with those reported for cultivated Chernozem WEOM (Qin et al. 2020), while the low HIX values (< 4) found for Steppe WEOM are similar to those of autochthonous aquatic OM (Ohno 2002; Huguet et al. 2009). Consequently, microbial products and poorly processed substances of plant origin predominate in the WEOM of uncultivated soil (Steppe). It was noted in a number of works that the properties and/or composition of WEOM weakly depend on the land use and management (Toosi et al. 2012), while others, on the contrary, found a strong impact of these factors on WEOM (Kalbitz et al. 2000). Our findings clearly show that the shape of the fluorescence spectra and the HIX index clearly differentiate the WEOM of Chernozems of contrasting land use.

The fluorescence index (FI) values are slightly higher for the LTBF samples (1.22–1.24) compared to Steppe (1.16–1.19), and according to two-way ANOVA, the differences are significant. Similarly, the BIX index is slightly higher for LTBF samples compared to the Steppe ones. FI and BIX are considered as indicators of the contribution of relatively fresh microbial OM. Unlike the expected negative correlation with the HIX index (Qin et al. 2020), FI and BIX in our case do not accurately reflect the features of the OM composition. This may be attributed to the geographical proximity of the experimental plots and the similar soil types as the sources of WEOM.

No significant dependence of HIX, BIX, and FI on salinity is observed for WEOM of both samples, but Steppe WEOM demonstrated a slight trend of HIX decreasing with increasing salinity.

Thus, the studied WEOM samples are best differentiated by the HIX index and shape of fluorescence spectra. Salinity increase leads to a decrease in the overall intensity of the fluorescence spectra of both WEOM samples, while the conventional fluorescence indices are insensitive to salinity changes.

3.4 Individual Fluorescent Components of WEOM

In the soil WEOM EEM spectra, three or four fluorescent components are most often identified by PARAFAC modeling (Sharma et al. 2017; Liu et al. 2019; Qin et al. 2020; Rinot et al. 2021). For both of our samples, the 5-component model best describes the array of spectral data for all salinity values. The spectra of five fluorescent components (C1, C2, C3, C4, and C5) obtained by PARAFAC analysis are shown in Fig. 4. Almost all components had one main emission maximum with two distinct excitation maxima. The identified components were assigned to the fluorophores typical for DOM by comparison with spectra from the library OpenFluor (https://openfluor.lablicate.com/of/measurement) based on high values of Tucker's congruence coefficient. A description of the components is given in Table 1.

The table illustrates the fact that spectra of components close to those obtained in this study are not always identified by different authors in the same way. Thus, components close to C1 are referred to as *humic like M* or *A peak*. In our opinion, this component is closer to the humic-like M-peak (Coble 1996; Coble et al. 2014).

The relative contributions of the PARAFAC components to the fluorescence spectra (fluorescence signature) of WEOM are little dependent on salinity, but differ markedly for Steppe and LTBF samples (Fig. 5). Noteworthy that the ratio between the contributions of fluorescent components in LTBF and Steppe samples in solution with different salinity remains almost constant. That is, the fluorescent signature of WEOM of the studied Chernozems does not change with increasing salinity.

Using PARAFAC modeling, we estimated the loadings of independent components to the fluorescence spectra of LTBF and Steppe WEOM samples with varying salinity. Component C1 was found to have the maximum loading for all experimental samples and was

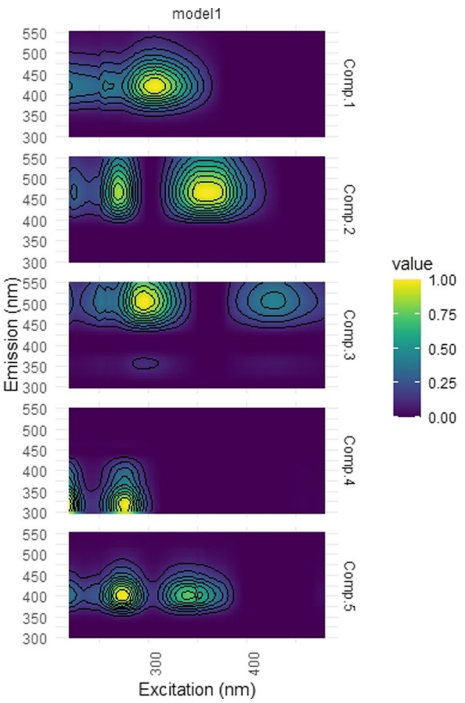

Fig. 4 The contour plots of EEM-PARAFAC components of WEOM of the experimental samples. Each EEM was normalized to its maximum fluorescence prior to modeling

Table 1 Description of individual fluorescent components identified by PARAFAC modeling in WEOM of Chernozems at all salinity values

Component #	Excitation wavelength, nm	Emission wavelength, nm	Description	Reference, Component ID
C1	305	420	Marine humic-like Biological activity and traditional peak M Marine humic-like, peak M (Coble 1996) or *microbial* Humic-like found in leaf leachates, potentially *bioavailable* Similar to humic A peak (Coble 1996) Humic-like M peak, *autochthonous, microbial*	(Chen et al. 2018) C2 (Lu et al. 2021) C5 (Gao and Gueguen 2016) C1 (Graeber et al. 2021) C4 (Søndergaard et al. 2003) C1 (Coble et al. 2014)
C2	360 (270)[a]	470	*Terrestrial* humic-like (close to peak C (Coble 1996) Terrestrial, humic-like, *allochthonous*	(Wünsch et al. 2018) C2 (Gao and Gueguen 2016) C3 (Walker et al. 2013) C2 (Coble et al. 2014)
C3	295 (425)	510 (355)	*Biodegradable* humic-like peak C+	(Wünsch et al. 2018) C6 (Sharma et al. 2017) C4 (Coble et al. 2014)
C4	275 (230)	320 (400)	*Protein-like fluorescence*, resembled the amino acids tryptophan and tyrosine (Coble 1996), containing fractions of autochthonous DOM (recent biological production) Mixture of polycyclic aromatic hydrocarbon (PAH) and protein-like substances, similar to peak N (Coble et al. 2014) Mix of humic-like component & tryptophan-like component	(Amaral et al. 2020b) C4 (Rinot et al. 2021) C4 (Amaral et al. 2020a) C5 (Amaral et al. 2021) C3 (Sharma et al. 2017) C3
C5	275 (340)	400	Terrestrial humic-like**,** *recalcitrant* Terrestrial humic-like Terrestrial humic material similar to the products of oxidative degradation of lignin Humic-like A_c	(Eder et al. 2022) C3 (Chen et al. 2018) C1 (Drozdova et al. 2022) C1 (Coble et al. 2014)

[a]Figures in brackets are for secondary maxima

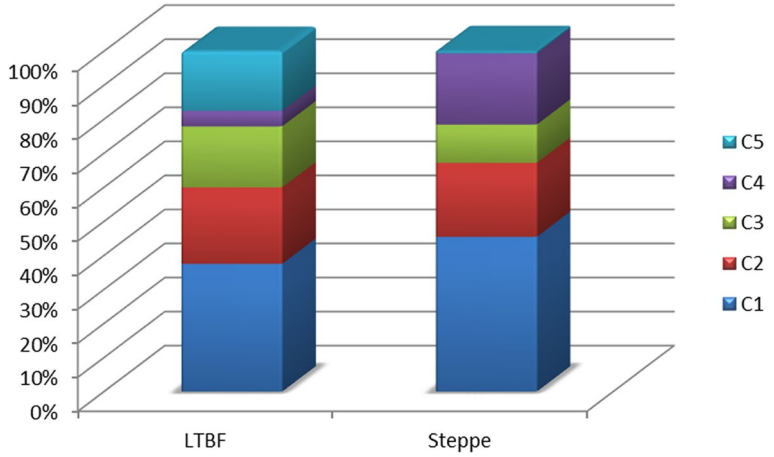

Fig. 5 Mean relative contributions of five fluorescence components to the overall fluorescence of LTBF and Steppe WEOM

identified as a humic-like autochthonous OM (Table 1). Its loading for LTBF WEOM was 0.42–0.47, and of the Steppe WEOM, it was about 0.58–0.61. This component is commonly found in DOM and WEOM samples and is considered as indicator of recent microbial activity (Coble et al. 2014), However, this component is usually not the most abundant in soil DOM (Sharma et al. 2017; Qin et al. 2020; Rinot et al. 2021; Eder et al. 2022). Even more surprisingly, in the spectra of LTBF WEOM, where microbial activity is attenuated, this component remains as dominant as in Steppe. This suggests that in Chernozems, this component may be correlated with OM of microbial origin in general. The second most abundant component, C2, was identified as humic-like allochthonous OM, which is one of the dominant components in the spectra of SOM, as well as freshwater and deep ocean OM (Ohno and Bro 2006; Ishii and Boyer 2012; Coble et al. 2014; Sharma et al. 2017). The C2 loadings to the spectra of both soil samples were very close, ranging from 0.25 to 0.29. The closeness of these values indicates a weak dependence of C2 on the land use, which is consistent with the findings of Williams et al. (2010). The third largest loading to the LTBF spectra was made by the C5 component (0.20–0.22), correlating with the most mature and stable aromatic OM (Eder et al. 2022). In the Steppe spectra, C4, representing protein-like fluorescence, was the third most significant component (0.26–0.29). The fourth most significant loading to the spectra of both soils, 0.2–0.23 — for LTBF and 0.14–0.15 — for Steppe, was made by C3, a humic-like component similar to C2 of (Sharma et al. 2017). This component is relatively rare in PARAFAC models, and based on the position of the maximum in the longest wavelength range, it characterizes the most decomposed OM, which is consistent with its larger fraction in the LTBF. The minor components, with fractions less than 0.1, were C4 in the LTBF WEOM spectra, which aligned with the decay of biological activity in this soil (Zhelezova et al. 2017), and C5 in the Steppe WEOM. The small loading of C5 to the Steppe WEOM is likely due to its accumulation only in cultivated soils, or its more effective stabilization in the Steppe. This stable and relatively hydrophobic OM is less sorbed on mineral particles compared to C2, and therefore, in the Steppe soil enriched with amphiphilic compounds of protein origin, C5 may be better stabilized and almost does not pass into the water extract. Furthermore, the C5 component is quite rare, as only three similar components were found in the OpenFluor database, and the

similarity scores for excitation and emission were reduced to 91% and 94%, respectively. Based on the calculated loadings of the components, their dependencies on salinity were plotted (Fig. 6).

The fluorescent components of LTBF WEOM, with the exception of protein-like C4, showed a dependence on salt concentration. The contribution of C1 at low concentrations of NaCl (0–1 g/L) was significantly higher than at high concentrations (10–35 g/L); however, a further increase from 1 to 35 mg/L had no significant effect. A similar trend can be observed for the C2 component, which is sensitive to the presence of NaCl, but reacts weakly to an increase in its concentration. Components C3 and C5 exhibited a more pronounced dependence on salt concentration up to 20 g/L, but a further increase in the NaCl content to 35 g/L did not significantly reduce their loadings to the spectra. For none of the PARAFAC components of LTBF WEOM, the load decreased to negligible values even at a salt concentration of 35 g/L.

In contrast to LTBF WEOM, the loadings of most of the fluorescent components of Steppe WEOM did not significantly depend on salinity. Only for the C4 component, the loading in the variant with the highest concentration of 35 g/L was significantly lower compared to the variant without NaCl adding. The contribution of C5 to the Steppe WEOM fluorescence was negligible at high salinity.

It should be noted that the isolated PARAFAC components for our samples mostly correlate well with the traditionally isolated peaks: C1 – M; C2 – C; C4 – B + T and C5 – A;

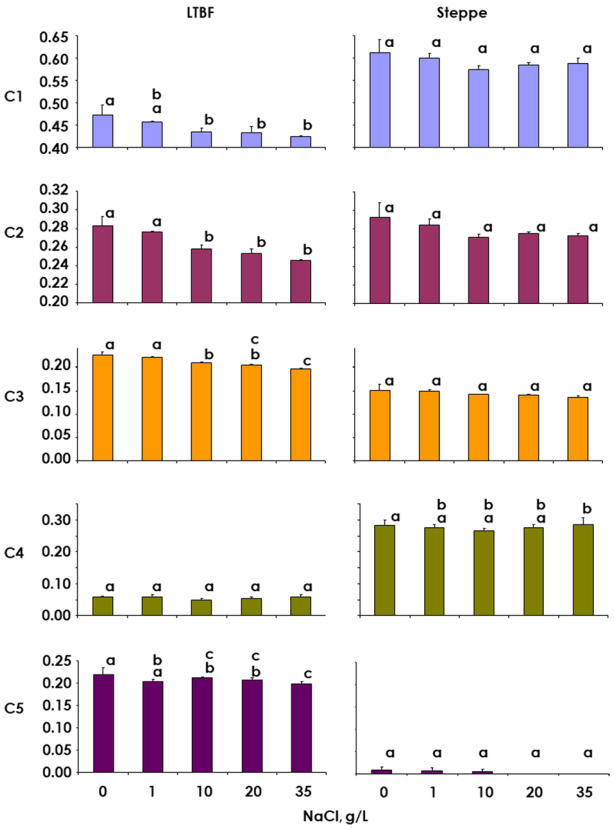

Fig. 6 Loadings of fluorescent components C1–C5 to the spectra of experimental samples at different salinities. The same letters denote means that do not differ significantly according to Tukey's test

accordingly, the same trends are observed for their proportions and salinity influence on them (Supplementary Information).

4 Conclusions

The findings of the study indicate that WEOM of Chernozem soils possesses high structural and aggregation resistance to salinity changes over a wide range of 0–35 g/L probably due to the unique characteristics of organic matter accumulation in these soils. DOC content remains constant with increasing salinity that means no aggregation or precipitation occurs.

Salinity variations had a rather weak effect on the absorption of WEOM of both soils. Minor but significant changes in $SUVA_{254}$, $S_{350\text{-}400}$, and S_R values occur only for the WEOM derived from LTBF soil. The fluorescence intensity for both Chernozem WEOM decreases with increasing salinity, but only for LTBF samples, the changes are significant. Overall, the observed changes in WEOM absorbance and fluorescence are evidently linked to alterations in the physicochemical structure, while the composition of OM remains unchanged.

Higher robustness of Steppe WEOM fluorescence can be attributed to its greater chemical diversity and enrichment with amphiphilic components promoting the persistence of its molecular ensemble. Probably, the protein-like fluorescent component C4, which is nearly five times more abundant in Steppe WEOM compared to LTBF extracts, may be partly responsible for this phenomenon.

While the optical indices show minimal differences among the WEOM of Chernozems with contrasting land use, significant variations are observed in their fluorescence spectra, humification index (HIX), and PARAFAC components loadings.

A distinctive feature of the WEOM fluorescence spectra of both Chernozems is the predominance of the C1 component resembling the traditional M peak associated with humic-like substances of marine origin and recent microbial activity. The components C3 and C5 are particularly specific to the WEOM of studied soils. Therefore, these two humic-like components hold promise as tracers for OM originated from typical Chernozem soils, especially those subjected to intensive cultivation. However, further investigations are necessary to evaluate the effects of photodegradation and to identify these components in fresh and marine waters.

Acknowledgements This work was supported by the Ministry of Science and Higher Education of the Russian Federation (Grant "Priority-2030" to Tomsk State University)

Author contributions [Vladimir A. Kholodov] contributed to conceptualization; [Nadezhda V. Yaroslavtseva] was involved in methodology; [Aliya R. Ziganshina] contributed to formal analysis and investigation; [Natalia N. Danchenko] was involved in writing — original draft preparation; [Vladimir A. Kholodov] contributed to writing — review and editing; and [Igor P. Semiletov] was involved in supervision.

Declarations

Competing interests The authors declare no competing interests.

References

Amaral V, Romera-Castillo C, Forja J (2020a) Dissolved organic matter in the Gulf of Cádiz: distribution and drivers of chromophoric and fluorescent properties. Front Mar Sci. https://doi.org/10.3389/fmars.2020.00126

Amaral V, Romera-Castillo C, García-Delgado M et al (2020b) Distribution of dissolved organic matter in estuaries of the southern Iberian Atlantic Basin: sources, behavior and export to the coastal zone. Mar Chem 226:103857. https://doi.org/10.1016/j.marchem.2020.103857

Amaral V, Romera-Castillo C, Forja J (2021) Submarine mud volcanoes as a source of chromophoric dissolved organic matter to the deep waters of the Gulf of Cádiz. Sci Rep 11:3200. https://doi.org/10.1038/s41598-021-82632-3

Barré P, Eglin T, Christensen BT et al (2010) Quantifying and isolating stable soil organic carbon using long-term bare fallow experiments. Biogeosciences 7:3839–3850. https://doi.org/10.5194/bg-7-3839-2010

Batjes N (2014) Total carbon and nitrogen in the soils of the world (EJSS Land Mark Paper No. 3). Eur J Soil Sci 47:151–163. https://doi.org/10.1111/ejss.12114_2

Bengtsson M, Attermeyer K, Catalán N (2018) Interactive effects on organic matter processing from soils to the ocean: are priming effects relevant in aquatic ecosystems? Hydrobiologia 822:1–17. https://doi.org/10.1007/s10750-018-3672-2

Bianchi T (2011) The role of terrestrially derived organic carbon in the coastal ocean: a changing paradigm and the priming effect. Proc Natl Acad Sci USA 108:19473–19481. https://doi.org/10.1073/pnas.1017982108

Borisover M, Lordian A, Levy G (2012) Water-extractable soil organic matter characterization by chromophoric indicators: effects of soil type and irrigation water quality. Geoderma 179–180:28–37. https://doi.org/10.1016/j.geoderma.2012.02.019

Boyd T, Barham B, Hall G, Osburn C (2010) Variation in ultrafiltered and LMW organic matter fluorescence properties under simulated estuarine mixing transects: 1. Mixing alone. J Geophys Res (biogeosciences). https://doi.org/10.1029/2009JG000992

Chantigny MH (2003) Dissolved and water-extractable organic matter in soils: a review on the influence of land use and management practices. Geoderma 113:357–380. https://doi.org/10.1016/S0016-7061(02)00370-1

Chen M, Park M, Kim J-H et al (2018) Exploring pore water biogeochemical characteristics as environmental monitoring proxies for a CO2 storage project in Pohang Basin, South Korea. Mar Pollut Bull. https://doi.org/10.1016/j.marpolbul.2018.10.036

Coble PG (1996) Characterization of marine and terrestrial DOM in seawater using excitation-emission matrix spectroscopy. Mar Chem 51:325–346. https://doi.org/10.1016/0304-4203(95)00062-3

Coble PG, Lead JR, Baker A et al (2014) Aquatic organic matter fluorescence. Cambridge University Press, Cambridge

Cole JJ, Prairie YT, Caraco NF et al (2007) Plumbing the global carbon cycle: integrating inland waters into the terrestrial carbon budget. Ecosystems 10:172–185. https://doi.org/10.1007/s10021-006-9013-8

Cuss CW, Donner MW, Noernberg T et al (2019) EEM-PARAFAC-SOM for assessing variation in the quality of dissolved organic matter: simultaneous detection of differences by source and season. Environ Chem 16:360–374

Danchenko NN, Artemyeva ZS, Kolyagin YG, Kogut BM (2020) Features of the chemical structure of different organic matter pools in Haplic Chernozem of the Streletskaya steppe: 13C MAS NMR study. Environ Res 191:110205. https://doi.org/10.1016/j.envres.2020.110205

Danchenko NN, Artemyeva ZS, Kolyagin YG, Kogut BM (2022) A comparative study of the humic substances and organic matter in physical fractions of Haplic Chernozem under contrasting land uses. Eurasian Soil Sci 55:1371–1383. https://doi.org/10.1134/S1064229322100039

Drozdova AN, Krylov IN, Nedospasov AA et al (2022) Fluorescent signatures of autochthonous dissolved organic matter production in Siberian shelf seas. Front Mar Sci. https://doi.org/10.3389/fmars.2022.872557

Eder A, Weigelhofer G, Pucher M et al (2022) Pathways and composition of dissolved organic carbon in a small agricultural catchment during base flow conditions. Ecohydrol Hydrobiol 22:96–112. https://doi.org/10.1016/j.ecohyd.2021.07.012

Endo S, Pfennigsdorff A, Goss K-U (2012) Salting-out effect in aqueous NaCl solutions: Trends with size and polarity of solute molecules. Environ Sci Technol 46:1496–1503. https://doi.org/10.1021/es203183z

Esteves VI, Santos EBH, Duarte AC (1999) Study of the effect of pH, salinity and DOC on fluorescence of synthetic mixtures of freshwater and marine salts. J Environ Monit 1:251–254. https://doi.org/10.1039/A902529D

Findlay S, Quinn J, Hickey C et al (2001) Effects of land use and riparian flowpath on delivery of dissolved organic carbon to streams. Limnol Oceanogr 46:345–355. https://doi.org/10.4319/lo.2001.46.2.0345

Franko U, Merbach I (2017) Modelling soil organic matter dynamics on a bare fallow Chernozem soil in Central Germany. Geoderma 303:93–98. https://doi.org/10.1016/j.geoderma.2017.05.013

Gao Z, Gueguen C (2016) Size distribution of absorbing and fluorescing DOM in Beaufort Sea, Canada Basin. Deep Sea Res Part i: Oceanogr Res Pap 121:1. https://doi.org/10.1016/j.dsr.2016.12.014
Gao Y, Yan M, Korshin G (2015) Effects of ionic strength on the chromophores of dissolved organic matter. Environ Sci Technol. https://doi.org/10.1021/acs.est.5b00601
Ghosh K, Schnitzer M (1980) Fluorescence excitation spectra of humic substances. Can J Soil Sci 60:373–379. https://doi.org/10.4141/cjss80-040
Gmach MR, Cherubin M, Kaiser K, Cerri CE (2020) Processes that influence dissolved organic matter in the soil: a review. Sci Agric 77:e20180164. https://doi.org/10.1590/1678-992X-2018-0164
Graeber D, Tenzin Y, Stutter M et al (2021) Bioavailable DOC: reactive nutrient ratios control heterotrophic nutrient assimilation—an experimental proof of the macronutrient-access hypothesis. Biogeochemistry 155:1–20. https://doi.org/10.1007/s10533-021-00809-4
Hansen AM, Kraus TEC, Pellerin BA et al (2016) Optical properties of dissolved organic matter (DOM): effects of biological and photolytic degradation. Limnol Oceanogr 61:1015–1032. https://doi.org/10.1002/lno.10270
Helms J, Stubbins A, Ritchie J et al (2008) Absorption spectral slopes and slope ratios as indicators of molecular weight, source, and photobleaching of chromophoric dissolved organic matter. Limnol Oceanogr 53:955–969. https://doi.org/10.2307/40058211
Huguet A, Vacher L, Relexans S et al (2009) Properties of fluorescent dissolved organic matter in the Gironde Estuary. Org Geochem 40:706–719. https://doi.org/10.1016/j.orggeochem.2009.03.002
Ishii SKL, Boyer TH (2012) Behavior of reoccurring PARAFAC components in fluorescent dissolved organic matter in natural and engineered systems: a critical review. Environ Sci Technol 46:2006–2017. https://doi.org/10.1021/es2043504
Kalbitz K, Solinger S, Park J-H et al (2000) Controls on the dynamics of dissolved organic matter in soils: a review. Soil Sci 165:277–304. https://doi.org/10.1097/00010694-200004000-00001
Karavanova EI (2013) Dissolved organic matter: fractional composition and sorbability by the soil solid phase (Review of literature). Eurasian Soil Sci 46:833–844. https://doi.org/10.1134/S1064229313080048
Kholodov VA, Yaroslavtseva NV, Farkhodov YuR et al (2019) Changes in the ratio of aggregate fractions in humus horizons of chernozems in response to the type of their use. Eurasian Soil Sci 52:162–170. https://doi.org/10.1134/S1064229319020066
Kholodov V, Yaroslavtseva N, Farkhodov Y et al (2020a) Optical properties of the extractable organic matter fractions in typical chernozems of long-term field experiments. Eurasian Soil Sci 53:739–748. https://doi.org/10.1134/S1064229320060058
Kholodov VA, Farkhodov YuR, Yaroslavtseva NV et al (2020b) Thermolabile and thermostable organic matter of chernozems under different land uses. Eurasian Soil Sci 53:1066–1078. https://doi.org/10.1134/S1064229320080086
Kothawala DN, Murphy KR, Stedmon CA et al (2013) Inner filter correction of dissolved organic matter fluorescence. Limnol Oceanogr Methods 11:616–630. https://doi.org/10.4319/lom.2013.11.616
Liu C, Li Z, Berhe AA et al (2019) Chemical characterization and source identification of organic matter in eroded sediments: Role of land use and erosion intensity. Chem Geol 506:97–112. https://doi.org/10.1016/j.chemgeo.2018.12.040
Lu K, Xu W, Yu H et al (2021) Insight into temporal–spatial variations of DOM fractions and tracing potential factors in a brackish-water lake using second derivative synchronous fluorescence spectroscopy and canonical correlation analysis. Environ Sci Eur 33:92. https://doi.org/10.1186/s12302-021-00538-3
Mann PJ, Spencer RGM, Hernes PJ et al (2016) Pan-arctic trends in terrestrial dissolved organic matter from optical measurements. Front Earth Sci. https://doi.org/10.3389/feart.2016.00025
McKnight DM, Boyer EW, Westerhoff PK et al (2001) Spectrofluorometric characterization of dissolved organic matter for indication of precursor organic material and aromaticity. Limnol Oceanogr 46:38–48. https://doi.org/10.4319/lo.2001.46.1.0038
Menichetti L, Houot S, van Oort F et al (2015) Increase in soil stable carbon isotope ratio relates to loss of organic carbon: results from five long-term bare fallow experiments. Oecologia 177:811–821
Mostofa K, Wu F, Liu C-Q et al (2011) Photochemical, microbial and metal complexation behavior of fluorescent dissolved organic matter in the aquatic environments. Geochem J 45:235–254. https://doi.org/10.2343/geochemj.1.0113
Murphy KR, Stedmon CA, Graeber D, Bro R (2013) Fluorescence spectroscopy and multi-way techniques. PARAFAC Anal Methods 5:6557–6566. https://doi.org/10.1039/C3AY41160E
Murphy KR, Stedmon CA, Wenig P, Bro R (2014) OpenFluor0—an online spectral library of auto-fluorescence by organic compounds in the environment. Anal Methods 6:658–661. https://doi.org/10.1039/C3AY41935E

Ohno T (2002) Fluorescence inner-filtering correction for determining the humification index of dissolved organic matter. Environ Sci Technol 36:742–746. https://doi.org/10.1021/es0155276
Ohno T, Bro R (2006) Dissolved organic matter characterization using multiway spectral decomposition of fluorescence landscapes. Soil Sci Soc Am J 70:2028–2037. https://doi.org/10.2136/sssaj2006.0005
Osadchiev A, Medvedev I, Shchuka S et al (2020) Influence of estuarine tidal mixing on structure and spatial scales of large river plumes. Ocean Sci 16:781–798. https://doi.org/10.5194/os-16-781-2020
Osburn CL, Del Vecchio R, Boyd TJ (2014) Physicochemical effects on dissolved organic matter fluorescence in natural waters. In: Baker A, Reynolds DM, Lead J et al (eds) Aquatic organic matter fluorescence. Cambridge University Press, Cambridge, pp 233–277
Patel-Sorrentino N, Mounier S, Benaim JY (2002) Excitation–emission fluorescence matrix to study pH influence on organic matter fluorescence in the Amazon basin rivers. Water Res 36:2571–2581. https://doi.org/10.1016/S0043-1354(01)00469-9
Piscart C, Genoel R, Doledec S et al (2009) Effects of intense agricultural practices on heterotrophic processes in streams. Environ Pollut 157:1011–1018. https://doi.org/10.1016/j.envpol.2008.10.010
Provenzano M, Cilenti A, Gigliotti G, Senesi N (2008) Spectroscopic investigation on hydrophobic and hydrophilic fractions of dissolved organic matter extracted from soils at different salinities. Clean: Soil, Air, Water 36:748–753. https://doi.org/10.1002/clen.200800033
Pucher M, Wünsch U, Weigelhofer G et al (2019) staRdom: versatile software for analyzing spectroscopic data of dissolved organic matter in R. Water. https://doi.org/10.3390/w11112366
Qin X, Yao B, Jin L et al (2020) Characterizing soil dissolved organic matter in typical soils from China using fluorescence EEM–PARAFAC and UV–visible absorption. Aquat Geochem 26:71–88. https://doi.org/10.1007/s10498-019-09366-7
Raymond PA, Spencer RGM (2015) Chapter 11—Riverine DOM. In: Hansell DA, Carlson CA (eds) Biogeochemistry of marine dissolved organic matter, 2nd edn. Academic Press, Boston, pp 509–533
Rinot O, Borisover M, Levy GJ, Eshel G (2021) Fluorescence spectroscopy: a sensitive tool for identifying land-use and climatic region effects on the characteristics of water-extractable soil organic matter. Ecol Ind 121:107103. https://doi.org/10.1016/j.ecolind.2020.107103
Rodrigues S, Trindade T, Duarte A et al (2015) A framework to measure the availability of engineered nanoparticles in soils: trends in soil tests and analytical tools. TrAC Trends Anal Chem. https://doi.org/10.1016/j.trac.2015.07.003
Sharma P, Laor Y, Raviv M et al (2017) Compositional characteristics of organic matter and its water-extractable components across a profile of organically managed soil. Geoderma 286:73–82. https://doi.org/10.1016/j.geoderma.2016.10.014
Søndergaard M, Stedmon C, Borch N (2003) Fate of terrigenous dissolved organic matter (DOM) in estuaries: aggregation and bioavailability. Ophelia 57:161–176. https://doi.org/10.1080/00785236.2003.10409512
Stedmon C, Markager S, Bro R (2003) Tracing dissolved organic matter in aquatic environments using a new approach to fluorescence spectroscopy. Mar Chem 82:239–254. https://doi.org/10.1016/S0304-4203(03)00072-0
Toosi ER, Castellano MJ, Singer JW, Mitchell DC (2012) Differences in soluble organic matter after 23 years of contrasting soil management. Soil Sci Soc Am J 76:628–637. https://doi.org/10.2136/sssaj2011.0280
Twardowski M, Boss E, Sullivan J, Donaghay P (2004) Modeling the spectral shape of absorbing chromophoric dissolved organic matter. Mar Chem 89:69–88. https://doi.org/10.1016/j.marchem.2004.02.008
Walker SA, Amon RMW, Stedmon CA (2013) Variations in high-latitude riverine fluorescent dissolved organic matter: a comparison of large Arctic rivers. J Geophys Res Biogeosci 118:1689–1702. https://doi.org/10.1002/2013JG002320
Williams CJ, Yamashita Y, Wilson HF et al (2010) Unraveling the role of land use and microbial activity in shaping dissolved organic matter characteristics in stream ecosystems. Limnol Oceanogr 55:1159–1171. https://doi.org/10.4319/lo.2010.55.3.1159
Wünsch U, Geuer J, Lechtenfeld O et al (2018) Quantifying the impact of solid-phase extraction on chromophoric dissolved organic matter composition. Mar Chem. https://doi.org/10.1016/j.marchem.2018.08.010
Zhelezova AD, Tkhakakhova AK, Yaroslavtseva NV et al (2017) Microbiological parameters of aggregates in typical chernozems of long-term field experiments. Eurasian Soil Sci 50:701–707. https://doi.org/10.1134/S1064229317060126
Zsolnay A (1996) Chapter 4—Dissolved humus in soil waters. In: Piccolo A (ed) Humic substances in terrestrial ecosystems. Elsevier, Amsterdam, pp 171–223

Zsolnay A, Baigar E, Jimenez M et al (1999) Differentiating with fluorescence spectroscopy the sources of dissolved organic matter in soils subjected to drying. Chemosphere 38:45–50. https://doi.org/10.1016/S0045-6535(98)00166-0